

# Role of layer packing for the electronic properties of the organic superconductor (BEDT-TTF)<sub>2</sub>Ag(CF<sub>3</sub>)<sub>4</sub>(TCE)

Michaela Altmeyer,<sup>\*</sup> Roser Valentí, and Harald O. Jeschke

*Institut für Theoretische Physik, Goethe-Universität Frankfurt, 60438 Frankfurt am Main, Germany*

(Received 27 March 2015; revised manuscript received 29 May 2015; published 16 June 2015)

The charge-transfer compound (BEDT-TTF)<sub>2</sub>Ag(CF<sub>3</sub>)<sub>4</sub>(TCE) crystallizes in three polymorphs with different alternating layers: While a phase with a  $\kappa$  packing motif has a low superconducting transition temperature of  $T_c = 2.6$  K, two phases with higher  $T_c$  of 9.5 and 11 K are multilayered structures consisting of  $\alpha'$  and  $\kappa$  layers. We investigate these three systems within density functional theory and find that the  $\alpha'$  layer shows different degrees of charge order for the two  $\kappa$ - $\alpha'$  systems and directly influences the electronic behavior of the conducting  $\kappa$  layer. We discuss the origin of the distinct behavior of the three polymorphs and propose a minimal tight-binding Hamiltonian for the description of these systems based on projective molecular Wannier functions.

DOI: [10.1103/PhysRevB.91.245137](https://doi.org/10.1103/PhysRevB.91.245137)

PACS number(s): 74.70.Kn, 71.20.Rv, 71.10.Fd, 71.15.Mb

## I. INTRODUCTION

For a few decades organic charge-transfer (CT) salts built of donor and acceptor molecular complexes have attracted a lot of attention due to the variety of ground states in their phase diagrams [1–5]. Application of external or chemical pressure can lead to antiferromagnetic insulating, charge ordered, spin-density wave, spin liquid, or unconventional superconducting ground states. Tendencies in the dimensionality of the electronic transport are often determined by the choice of conducting molecules: Compounds containing TMTTF (tetramethyltetrathiafulvalene) molecules, for example, are typically one dimensional [1,5], whereas several phases of BEDT-TTF (bisethylenedithio-tetrathiafulvalene) based salts show two-dimensional behavior. However, the arrangement of the (donor) molecules in these complexes is decisive. Among the BEDT-TTF family of CT salts, many different packings classified as  $\alpha$ ,  $\alpha'$ ,  $\beta$ ,  $\beta'$ ,  $\beta''$ ,  $\delta$ ,  $\kappa$ , and  $\theta$  have been experimentally realized and a wide range of different physical properties was found [6–9]. Depending on the preparation conditions, different polymorphs of one structure can be synthesized; for example, (BEDT-TTF)<sub>2</sub>I<sub>3</sub> crystallizes in  $\alpha$ ,  $\beta$ ,  $\theta$ , and  $\kappa$  forms [10]. Polymorphs provide an opportunity to explore the influence of the packing motif on the electronic properties. Effects originating from differences in the anion layer composition can be excluded in this case since this layer remains unaltered in the polymorph family.

Here we consider the polymorph charge-transfer salt family (BEDT-TTF)<sub>2</sub>Ag(CF<sub>3</sub>)<sub>4</sub>(TCE) (see Fig. 1) first synthesized by Schlueter and collaborators [11]. TCE stands for 1,1,2-trichloroethane and in the following we will make use of the common abbreviation ET for BEDT-TTF. These systems show a metallic behavior at low temperatures and a  $T_c$  of 2.6 K to a superconducting state was measured for the single-layered compound [Fig. 1 (a)] where the ET molecules form dimers arranged in a so-called  $\kappa$  pattern. The term  $\kappa_L$  phase was coined for this structure, with the index  $L$  referring to the low  $T_c$ . Structural refinement of the other two multiphase polymorphs [12,13] [Figs. 1(b), 1(c), and 2] showed the presence of charge-ordered layers in  $\alpha'$  packing between the

$\kappa$ -type layers;  $\alpha'$  phases have also been characterized as Mott-Hubbard insulators [14–16]. Even though as insulating layers they do not contribute directly to superconductivity, their existence seems to enhance the superconducting transition temperature in (BEDT-TTF)<sub>2</sub>Ag(CF<sub>3</sub>)<sub>4</sub>(TCE). While the dual-layered  $\kappa$ - $\alpha'_1$  compound exhibits superconductivity at a critical temperature of 9.5 K, which is approximately 3.5 times higher than the  $T_c$  of the  $\kappa_L$  phase, the four-layered  $\kappa$ - $\alpha'_2$  phase shows superconductivity at 11 K and therefore belongs to the organic superconductors with the highest measured critical temperatures.

In this work we perform density functional theory (DFT) calculations for the three polymorphs. We especially focus on the effects of the  $\alpha'$  layers on the electronic properties of the  $\kappa$  layers in the dual and four-layered systems and perform a comparative analysis of the three systems in terms of *ab initio* derived tight-binding Hamiltonians using the projective Wannier method. While all three systems show apparently similar  $\kappa$  bands, the charge ordering in the  $\alpha'$  layer in  $\kappa$ - $\alpha'_1$  and  $\kappa$ - $\alpha'_2$  influences significantly the magnitude of the hoppings in the conducting  $\kappa$  layer. Analysis of the degree of frustration within a minimal triangular lattice model hints to the different superconducting  $T_c$  in these systems.

## II. CRYSTAL STRUCTURE

### A. $\kappa$ phase

The single-layered phase crystallizes in the orthorhombic  $Pnma$  space group and its unit cell contains two donor layers which are separated by an insulating layer consisting of the anion [Ag(CF<sub>3</sub>)<sub>4</sub>]<sup>−</sup> and the solvent TCE [17]. However, the anion layer is disordered. In order to simplify the density functional theory calculations we choose one of the two symmetry-allowed orientations of the anion and lower the symmetry to  $P2_1/c$  (no. 14); the corresponding simplified structure is shown in Fig. 1(a). Note that for better comparability with the  $\kappa$ - $\alpha'_1$  and  $\kappa$ - $\alpha'_2$  phases we denote with  $a$  the short in-plane axis, with  $b$  the long in-plane axis and with  $c$  the stacking direction (even though the original  $Pnma$  structure has a  $b$  stacking direction). In the two donor layers, the ET molecules are in the  $\kappa$  packing motif [see Fig. 3(a)] but with

<sup>\*</sup>altmeyer@itp.uni-frankfurt.de

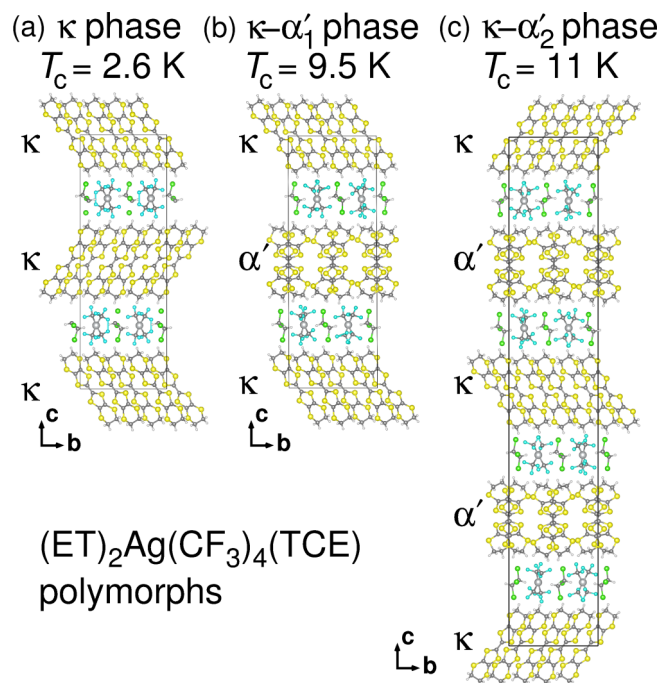


FIG. 1. (Color online) Crystal structures of the three polymorphs of (BEDT-TTF)<sub>2</sub>Ag(CF<sub>3</sub>)<sub>4</sub>(TCE).

alternating tilt of the molecules with respect to the acceptor layer.

### B. $\kappa$ - $\alpha'_1$ phase

The triclinic crystal structure  $P\bar{1}$  of the dual-layered compound is shown in Fig. 1(b). Compared to the single-layered phase, the layer in the center of the unit cell is here replaced by an  $\alpha'$  packed layer. This packing motif is characterized by molecules that are lined up on a rectangular lattice [see Figs. 2 and 3(c)]. The rows of molecules along  $b$  alternate between a right and a left tilt with respect to the

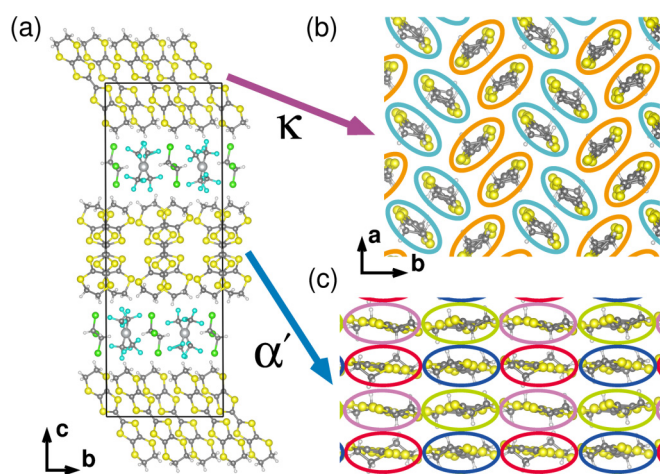


FIG. 2. (Color online) Crystal structure of  $\kappa$ - $\alpha'_1$ -(BEDT-TTF)<sub>2</sub>Ag(CF<sub>3</sub>)<sub>4</sub>(TCE) together with cuts illustrating the two alternating ET patterns. In (b) and (c), colored outlines mark symmetry inequivalent ET molecules.

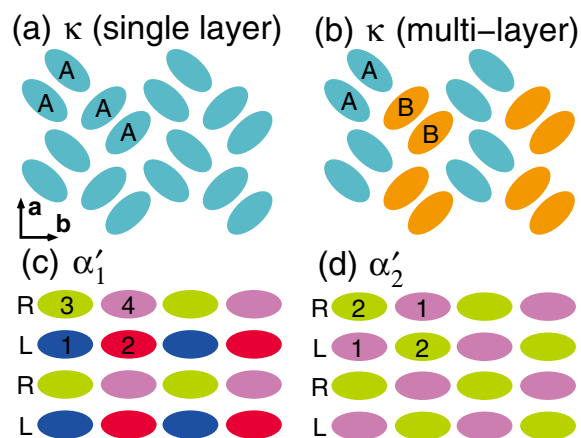


FIG. 3. (Color online) Schematic of BEDT-TTF molecule arrangement in the considered materials. (a)  $\kappa$ -type packing in the low  $T_c$  (BEDT-TTF)<sub>2</sub>Ag(CF<sub>3</sub>)<sub>4</sub>(TCE) compound. (b)  $\kappa$ -type packing in the two high  $T_c$  compounds.  $\alpha'_1$ -type packing in the two-layer compound. (c)  $\alpha'_1$ -type packing in the four-layer compound. Symmetry inequivalent molecules are marked by numbers and colored differently. R (L) indicate tilting of the molecules to the right (left) in the  $\alpha'$  layers.

$a$  axis. This leads to the characteristic cross pattern when viewed along  $a$  [Figs. 2 and 3(c)]. In contrast to other  $\alpha'$  packed structures [8], no dimerization and therefore also no shift along the long unit-cell axis has been observed. The low symmetry of the space group means that in the  $\kappa$  layer the two ET molecules in a dimer are still related by inversion symmetry but there are two symmetry inequivalent dimers, and in the  $\alpha'$  layer there are even four inequivalent ET molecules [see Figs. 2, 3(b), and 3(c)].

### C. $\kappa$ - $\alpha'_2$ phase

The polymorph with the highest superconducting critical temperature has the largest unit cell [13,18,19], where two  $\kappa$  layers alternate with two  $\alpha'$  layers [Fig. 1(c)]. Due to the monoclinic  $P2_1/n$  symmetry (space group no. 14), every second  $\kappa$  ( $\alpha'$ ) layer is shifted by half the lattice vector  $a$ . Note that DFT codes usually allow only one setting of space group no. 14; we therefore perform the calculations in a  $P2_1/c$  setting. As in the case of  $\kappa$ - $\alpha'_1$ , the monoclinic space group leads to two symmetry inequivalent (ET)<sub>2</sub> dimers in the  $\kappa$  layer; the two ET molecules in a dimer are related by inversion symmetry [see Fig. 3(b)]. The symmetry also leads to a checkerboard pattern of symmetry related ET molecules in the  $\alpha'$  layer as displayed in Fig. 3(d).

## III. ELECTRONIC STRUCTURE

We determine the electronic structure of (BEDT-TTF)<sub>2</sub>Ag(CF<sub>3</sub>)<sub>4</sub>(TCE) using the all electron full potential local orbital basis as implemented in the FPLO code [20] and the generalized gradient approximation functional [21]. A  $6 \times 6 \times 6$   $k$  mesh was employed to converge the energy and charge density.

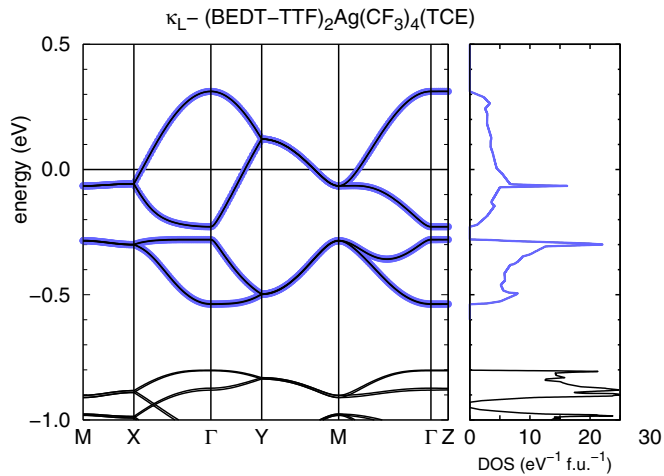


FIG. 4. (Color online) DFT band structure and density of states of the  $\kappa$  phase. The blue bands are determined by the projective Wannier function method and originate from the ET HOMO orbitals.

### A. $\kappa$ phase

The band structure and density of states (DOS) of the  $\kappa$  phase are presented in Fig. 4. There are eight bands in the energy window  $[-0.6\text{ eV}, 0.4\text{ eV}]$  deriving exclusively from the highest occupied molecular orbitals (HOMOs) of the eight ET molecules in the unit cell. As there is only a very small dispersion in the stacking direction ( $\Gamma$ - $Z$  path) the bands originating from the two layers in the unit cell are almost degenerate. The dimerization of the ET molecule pairs is reflected in the bonding ( $[-0.6\text{ eV}, -0.3\text{ eV}]$ ) and antibonding ( $[-0.3\text{ eV}, 0.4\text{ eV}]$ ) character of the bands. The band structure of  $\kappa - (\text{BEDT-TTF})_2\text{Ag}(\text{CF}_3)_4(\text{TCE})$  is very similar to  $\kappa - (\text{BEDT-TTF})_2X$  compounds with other anions  $X$  [22,23]. Integrating the partial densities of states for symmetry inequivalent molecules in the range  $[-0.6, 0]$  eV results in a charge transfer of one hole per  $(\text{ET})_2$  dimer to the anion layer.

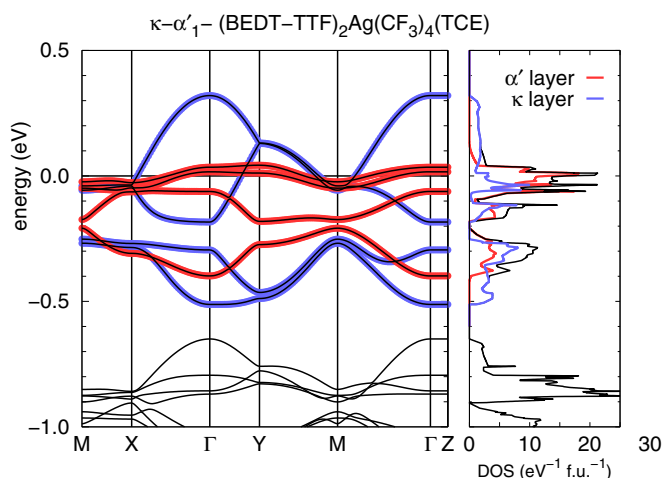


FIG. 5. (Color online) Band structure and density of states (DOS) of the  $\kappa$ - $\alpha'_1$  phase. The Wannier bands (blue symbols for  $\kappa$  orbitals and red symbols for  $\alpha'$  orbitals) are in excellent agreement with the DFT bands.

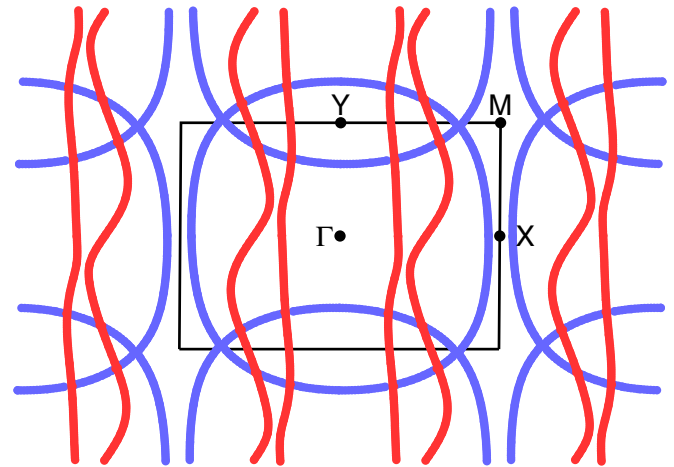


FIG. 6. (Color online) Calculated Fermi surface of the dual layered compound: The elliptical shapes in blue are due to the bands arising from the ET molecules of the  $\kappa$  layer, while the wiggly lines in red are the almost one-dimensional features resulting from the  $\alpha'$  layer.

### B. $\kappa$ - $\alpha'_1$ phase

In Fig. 5 we show the band structure and layer-resolved density of states of the dual-layered compound. The anion layer has no weight at the Fermi level and therefore does not contribute to the electronic transport. The bands originating from the  $\kappa$  layer are similar in shape to the bands of the  $\kappa$  phase (Fig. 4) while the  $\alpha'$  bands are narrower and less dispersive than the  $\kappa$  bands. The corresponding Fermi surface of the  $\kappa$ - $\alpha'_1$  phase is shown in Fig. 6. Here, the elliptical shape corresponds to the  $\kappa$  layer and is typical for this packing motif [22,24]. In contrast, the  $\alpha'$  Fermi surface (wiggly lines in Fig. 6) is quasi-one-dimensional and has no dispersion in the  $k_z$  direction.

Recent de Haas-van Alphen experiments for the dual-layered compound observed only elliptic orbitals originating from the  $\kappa$  bands [19] and, as expected, no  $\alpha'$  bands were detected. However, one should mention that on the one hand

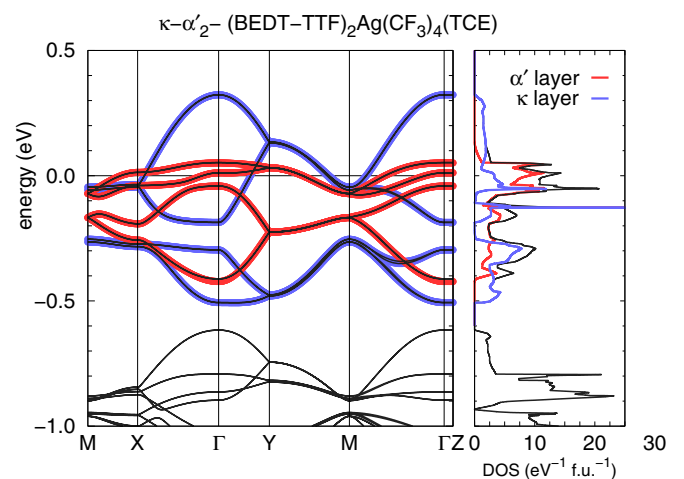


FIG. 7. (Color online) Band structure and density of states of the  $\kappa$ - $\alpha'_2$  phase. The DFT band structure is shown with black lines, while the Wannier bands are displayed with blue ( $\kappa$ ) and red ( $\alpha'$ ) symbols.

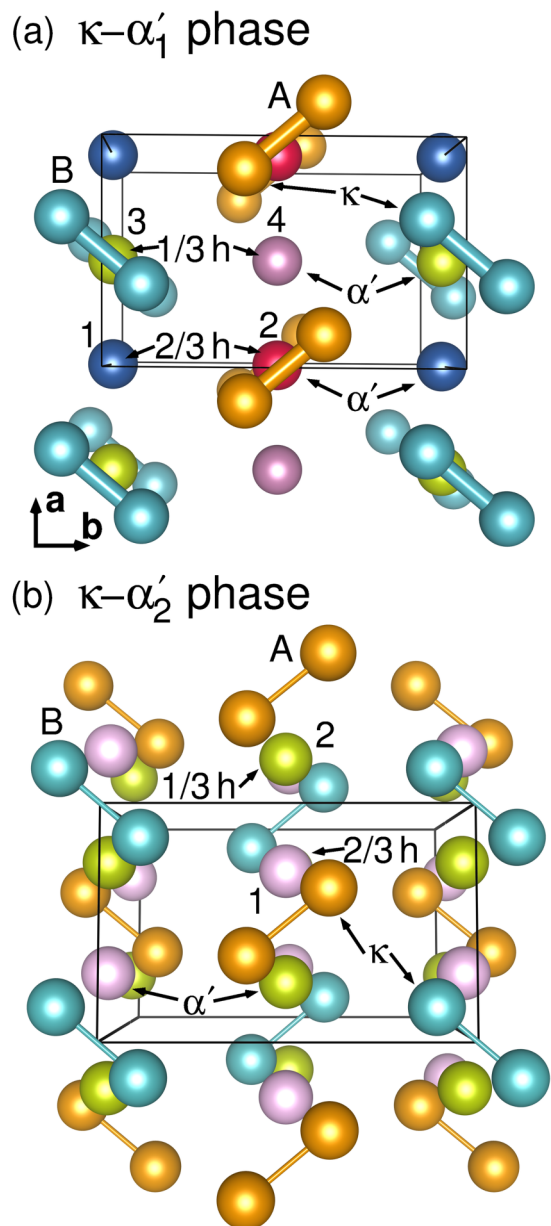


FIG. 8. (Color online) Illustration of the two different  $\kappa$  dimers in the charge ordered environment as created by the  $\alpha'$  layer in the  $\kappa$ - $\alpha'_1$  and  $\kappa$ - $\alpha'_2$  phase. ET molecules are shown as spheres; the two symmetry inequivalent  $\kappa$  layer ET molecules are labeled A and B. (a) The four inequivalent  $\alpha'$  layer ET molecules in the  $\kappa$ - $\alpha'_1$  phase carry numbers 1 through 4. (b) There are only two inequivalent  $\alpha'$  layer molecules in the  $\kappa$ - $\alpha'_2$  phase that are labeled 1 and 2.

the  $\alpha'$  packed systems have been reported in the past as Mott-Hubbard insulators [14–16] and, on the other hand, DFT underestimates correlation effects and cannot reproduce the insulating behavior of a Mott system. A better treatment of correlations beyond DFT in organic materials [25] (presently beyond the scope of this study) could lead to an opening of a gap at the Fermi level in the  $\alpha'$  bands and to a Fermi surface with only  $\kappa$  bands. Note, however, that direct hybridization between  $\alpha'$  and  $\kappa$  layers is almost negligible (maximum  $\alpha'$  to  $\kappa$  hopping parameters in  $\kappa$ - $\alpha'_1$  and  $\kappa$ - $\alpha'_2$  are 0.2–0.3 meV) so that it is justified to focus our investigation on the properties of the  $\kappa$  layers even in  $\kappa$ - $\alpha'_1$  and  $\kappa$ - $\alpha'_2$  as these layers will be responsible for the observed superconductivity.

The charge transfer in this system has more features than in the pure  $\kappa$  phase compound due to the low symmetry and the presence of the  $\alpha'$  layer. We find that the right tilted ET molecules in the  $\alpha'$  plane contribute a charge of the order of 1/3 electron [0.343 for ET molecule 3 as denoted in Fig. 3(c) and 0.316 for molecule 4]. The other two left tilted molecules show a larger charge transfer of the order of 2/3 of an electron (0.658 for molecule 1 and 0.705 for molecule 2). For clarity, we depict in Fig. 8(a) this charge ordering. A similar charge disproportionation has already been observed in other  $\alpha'$  charge transfer salts (e.g., in  $\alpha'$ -ET<sub>2</sub>Ag(CN)<sub>2</sub> [26]), where the homogeneous charge transfer of the ET molecules at high temperature is redistributed to a 1/3 versus 2/3 order upon cooling.

In the  $\kappa$  layer, the symmetry of the crystal leads to two symmetry inequivalent (ET)<sub>2</sub> dimers with distances between the ET molecules in a dimer of  $d_A = 3.74\text{\AA}$  and  $d_B = 3.77\text{\AA}$ . However, the charge transfer from these dimers to the anion layer is the same within the computational accuracy—0.493 electrons for ET molecule A [see Fig. 3(b)] and 0.494 for molecule B.

### C. $\kappa$ - $\alpha'_2$ phase

Figure 7 shows the band structure and density of states of the four-layered compound. As the unit cell consists of four donor layers, there are 16 bands corresponding to the HOMOs of the ET molecules. However, as the dispersion along the stacking direction is extremely small, the bands originating from the two identically packed layers in the unit cell are nearly pairwise degenerate and the band structure is very similar to that of the  $\kappa$ - $\alpha'_1$  compound (see Appendix B). Nevertheless, the subtle quantitative differences between the electronic structure of the two systems, in particular in the  $\alpha'$  bands, have important consequences on the behavior of the materials as it is reflected,

TABLE I. Tight-binding parameters for the  $\kappa$  layers of all three phases. Distances between ET molecule centers are listed for identification of hopping paths.

System		$t_0^A$	$t_0^B$	$t_1^A$	$t_1^B$	$t_2^A$	$t_2^B$	$t_3^A$	$t_3^B$	$t_4^A$	$t_4^B$
$\kappa$	$t_i$ (meV)	−181.3		168.0		102.4		60.8		33.4	
	$d_i$ (Å)	0		3.78		5.55		6.79		6.73	
$\kappa$ - $\alpha'_1$	$t_i$ (meV)	−166.7	−159.7	170.4	161.0	−98.8	−96.3	64.1	67.6	−38.1	−32.4
	$d_i$ (Å)	0	0	3.74	3.77	5.60	5.65	6.64	6.66	6.84	6.85
$\kappa$ - $\alpha'_2$	$t_i$ (meV)	−164.4	−162.5	166.0	163.2	−98.7	−98.1	70.5	62.9	−35.0	−37.6
	$d_i$ (Å)	0	0	3.73	3.76	5.64	5.59	6.61	6.67	6.83	6.83

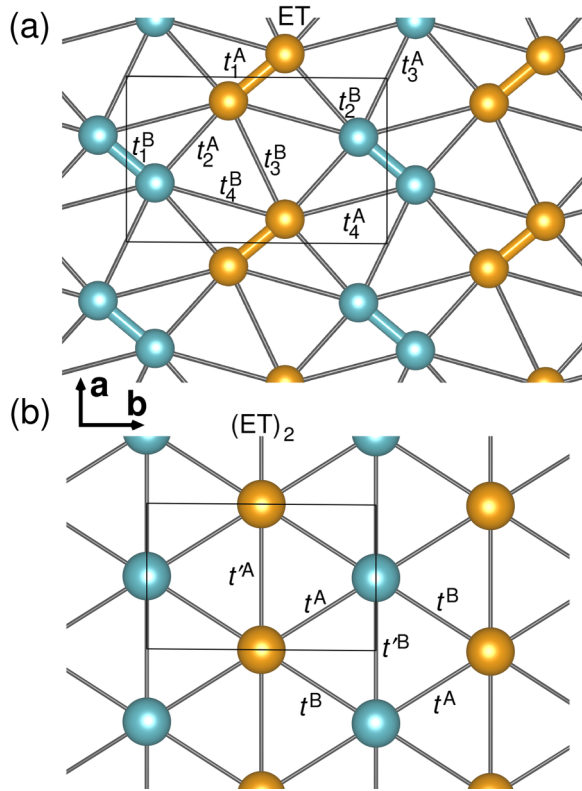


FIG. 9. (Color online) (a) Illustration of the eight nearest-neighbor hopping paths in the molecule model for the layer of the dual-layered phase. (b) Illustration of the tight-binding parameters of the dimer model.

for instance, in the charge transfer. The  $P2_1/c$  symmetry in  $\kappa\text{-}\alpha'_2$  poses stronger restrictions on the charge transfer in the  $\alpha'$  layer compared to the  $P\bar{1}\kappa\text{-}\alpha'_1$  system. The symmetry equivalent ET molecules form a checkerboard pattern on the rectangular lattice as shown in Fig. 3(d). The ET molecules on one of the  $\alpha'$  sublattices donate 0.367 electrons, while the other molecules transfer approximately 0.611 electrons. Thus, the average charge transfer from the  $\alpha'$  layers to the anion layer is slightly less than half an electron per ET molecule.

As in the  $\kappa\text{-}\alpha'_1$  system, there are two symmetry inequivalent  $(\text{ET})_2$  dimers in the  $\kappa$  layer. The distances of the molecules within the dimers differ slightly, at  $d_A = 3.73 \text{ \AA}$  and  $d_B = 3.76 \text{ \AA}$ . There is a small charge disproportionation between the dimers, with ET molecules of dimer A transferring 0.520 electrons to the anion, while those of dimer B transfer 0.500 electrons [compare Fig. 3(b)]. Thus, the  $\kappa$  layer compensates for the slightly too low charge transfer of the  $\alpha'$  layer.

An important difference between the  $\kappa\text{-}\alpha'_1$  and  $\kappa\text{-}\alpha'_2$  phases is that the constraint imposed by the higher symmetry in  $\kappa\text{-}\alpha'_2$

translates into a more symmetric charge order in the  $\alpha'$  layer in  $\kappa\text{-}\alpha'_2$  than in  $\kappa\text{-}\alpha'_1$  and the corresponding  $\alpha'\text{-}\kappa$  stacking in  $\kappa\text{-}\alpha'_2$  shows the center of the  $(\text{ET})_2$  dimers of the  $\kappa$  layers always aligned between the two differently charged ET molecules in the  $\alpha'$  layer [Fig. 8(b)], contrary to what happens in  $\kappa\text{-}\alpha'_1$ . Note that the further inclusion of correlations may change the degree of charge order while the symmetry constraints will keep the pattern the same. This charge arrangement has important consequences on the Hamiltonian description of these systems as we show below.

#### IV. TIGHT-BINDING HAMILTONIAN

We use the projective Wannier function method as implemented in FPLO [27] in order to obtain the tight-binding parameters for the conducting  $\kappa$  layers in  $(\text{BEDT-TTF})_2\text{Ag}(\text{CF}_3)_4(\text{TCE})$  from Wannier function overlaps. Considering the central point of the inner C–C bond of the ET molecules as sites, the tight-binding (TB) Hamiltonian can be written as

$$H = \sum_{ij,\sigma} t_{ij}(c_{i\sigma}^\dagger c_{j\sigma} + c_{j\sigma}^\dagger c_{i\sigma}), \quad (1)$$

where  $c_{i\sigma}^\dagger$  ( $c_{i\sigma}$ ) creates (destroys) an electron on site  $i$ .

When the dimerization of the ET molecule pairs is strong, the separation between bonding and antibonding bands is large and the analysis of the low-energy tight-binding Hamiltonian can be reduced to the two partially occupied antibonding bands. This case corresponds to a half-filled anisotropic triangular lattice where the sites denote the centers of the  $(\text{ET})_2$  dimers (centers of the two inner C–C bonds on neighboring ET molecules):

$$H = \sum_{(ij),\sigma} t(c_{i\sigma}^\dagger c_{j\sigma} + c_{j\sigma}^\dagger c_{i\sigma}) + \sum_{[ij],\sigma} t'(c_{i\sigma}^\dagger c_{j\sigma} + c_{j\sigma}^\dagger c_{i\sigma}). \quad (2)$$

$t$  and  $t'$  correspond to nearest- and next-nearest-neighbor hopping contributions. The hoppings between dimers [Eq. (2)] can be connected to the hoppings between molecules [Eq. (1)] using geometrical as well as analytical considerations [7,22,28,29]:

$$t \approx \frac{|t_2| + |t_4|}{2} \quad \text{and} \quad t' \approx \frac{|t_3|}{2}. \quad (3)$$

Here  $t_2$  and  $t_4$  are the hoppings between one molecule and the two closest molecules on the orthogonal oriented dimer.  $t_3$  belongs to the hopping between the closest ET molecules on neighboring equally oriented dimers.

In Table I we list the hopping parameters between ET molecules [Eq. (1) and Fig. 9(a)] in the  $\kappa$  layer of the three polymorphs  $(\text{BEDT-TTF})_2\text{Ag}(\text{CF}_3)_4(\text{TCE})$ . Due to the

TABLE II. Tight-binding parameters for the  $\alpha'$  layers of the dual-layered phase. Distances between ET molecule centers are listed for identification of hopping paths.

System		$t_0^1$	$t_0^2$	$t_0^3$	$t_0^4$	$t_1^{13}$	$t_1^{24}$	$t_2^{12}$	$t_2^{34}$	$t_3^{14}$	$t_3^{23}$	$t_4^{14}$	$t_4^{23}$
$\kappa\text{-}\alpha'_1$	$t_i$ (meV)	−55.9	−36.3	−189.1	−145.9	69.9	43.0	−9.5	−66.1	26.2	21.9	11.3	3.3
	$d_i$ (Å)	0	0	0	0	4.21	4.21	6.61	6.61	7.81	7.81	7.86	7.86

TABLE III. Tight-binding parameters for the  $\alpha'$  layers of the four-layered phase. Distances between ET molecule centers are listed for identification of hopping paths.

System		$t_0^1$	$t_0^2$	$t_1$	$t_2$	$t_3$	$t_4$	$t_5$	$t_6$	$t_7$	$t_8$
$\kappa\text{-}\alpha'_2$	$t_i$ (meV)	-90.2	-126.9	47.2	73.5	-35.0	-70.1	30.9	31.4	9.6	12.5
	$d_i$ (Å)	0	0	4.16	4.24	6.60	6.61	7.61	7.66	7.99	8.04

presence of two inequivalent  $(\text{ET})_2$  dimers in  $\kappa\text{-}\alpha'_1$  and  $\kappa\text{-}\alpha'_2$ , these phases have twice as many TB parameters compared to the  $\kappa$  phase. For the  $\kappa$ -only system, the approximate symmetry of  $P2_1/c$  we employ means that  $\kappa$  molecules are all equivalent within the layer but inequivalent between neighboring layers; however, as differences between TB parameter sets are below 0.3 meV, we report only one of them in Table I. Note that the absolute value of the TB parameters depends on the strength of the overlap of the Wannier orbitals and is very sensitive to variations in the distance and the orientation of the ET molecules, while the sign originates from the phase factors of the TB Hamiltonian. For completion, we also show in Tables II and III the hopping parameters between ET molecules in the  $\alpha'$  layer for  $\kappa\text{-}\alpha'_1$  and  $\kappa\text{-}\alpha'_2$ , respectively. We observe that the different charge distribution among the ET molecules in the  $\alpha'$  layers is a manifestation of the different crystal-field environment of the molecules as quantified by the onsite parameters ( $t_0$ ) in Tables II and III. In Table IV, the tight-binding parameters for the dimer model [Eq. (2) and Fig. 9(b)] are listed.

A detailed analysis on the hopping parameters for  $\kappa\text{-}\alpha'_1$  in Table I shows that the tight-binding parameters differentiate between the two inequivalent  $(\text{ET})_2$  dimers and reflect the stripy charge transfer found for the  $\alpha'$  layer and illustrated in Fig. 8(a). The more tightly bound dimers (A) are above the stronger charged  $\alpha'$  ET molecules with a  $2/3$  hole; the less tightly bound dimers (B) are above the weakly charged  $\alpha'$  ET molecules with a  $1/3$  hole.

In  $\kappa\text{-}\alpha'_2$  the strength of the dimerization as defined by the size of the intradimer hoppings  $t_1^A$  and  $t_1^B$  is on average slightly smaller than in the other two polymorphs. Here, contrary to the  $\kappa\text{-}\alpha'_1$  case, the TB parameters do not show the stripy pattern from  $\kappa\text{-}\alpha'_1$  since both the A and B  $(\text{ET})_2$  dimers are aligned between the two distinctly charged ET molecules in the  $\alpha'$  layer [see Fig. 8(b)].

In all three polymorphs, the dimer model estimate [Eq. (2)] does not give such a good representation of the band structure (see Appendix A) as, for instance, in  $\kappa\text{-}(\text{ET})_2\text{Cu}_2(\text{CN})_3$  [22,23]. This may partly be due to the weak degree of dimerization in  $(\text{BEDT-TTF})_2\text{Ag}(\text{CF}_3)_4(\text{TCE})$ , but more importantly it reflects the fact that the basis defined by the hoppings between dimer sites is not rich enough to correctly describe details

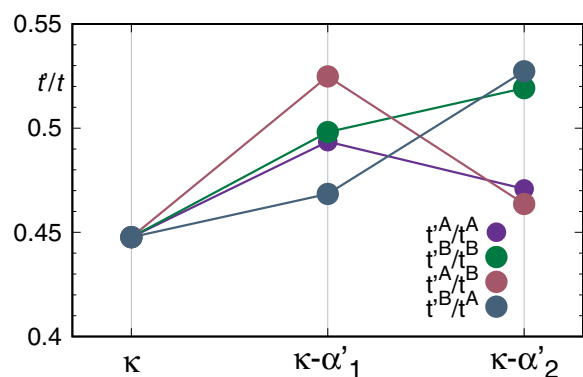
 TABLE IV. Table of triangular lattice Hamiltonian parameters  $t$  and  $t'$  for the three polymorphs, given in meV.

System	$t^A$	$t^B$	$t'^A$	$t'^B$
$\kappa$		67.9		30.4
$\kappa\text{-}\alpha'_1$	-68.4	-64.4	33.8	32.1
$\kappa\text{-}\alpha'_2$	-66.8	-67.9	31.5	35.2

of the band structure and Fermi surface. Only by allowing the larger basis defined by the hopping amplitudes between molecules can all relevant details be captured. Keeping in mind that the dimer model only provides an approximate representation of the band structures, we use it to roughly compare the obtained trends to other previously examined  $\kappa$  structures. The frustration is given by the ratio of the next-nearest hopping to the nearest hopping  $|t'/t|$ . Figure 10 shows that for the multilayered phases  $|t'/t| \approx 0.5$ , which is close to the value 0.58 obtained for  $\kappa\text{-}(\text{ET})_2\text{Cu}(\text{SCN})_2$  [22], which is superconducting at a temperature of 10.4 K. The low  $T_c$   $\kappa$  phase is less frustrated and the frustration parameter of 0.45 is just slightly higher than the one calculated for the antiferromagnetic insulator  $\kappa\text{-}(\text{BEDT-TTF})_2\text{Cu}[\text{N}(\text{CN})_2]\text{Cl}$ .

## V. DISCUSSION AND CONCLUSIONS

Our microscopic analysis of the polymorph family  $(\text{BEDT-TTF})_2\text{Ag}(\text{CF}_3)_4(\text{TCE})$  with density functional theory and projective Wannier function derived tight-binding Hamiltonians showed that, even though the  $\alpha'$  layer in these materials is most probably insulating, its electronic structure decisively influences the behavior of the conducting  $\kappa$  layer in  $\kappa\text{-}\alpha'_1$  and  $\kappa\text{-}\alpha'_2$ . In particular, the TB hopping parameters in  $\kappa\text{-}\alpha'_1$  reflect the stripe-like charge order pattern shown by the ET molecules in the  $\alpha'$  layer. In  $\kappa\text{-}\alpha'_2$  there is no such pattern since the  $(\text{ET})_2$  dimers in  $\kappa\text{-}\alpha'_2$  are always aligned between the two distinctly charged ET molecules in the  $\alpha'$  layer. This different charge arrangement has its origin on the symmetry constraint imposed by  $P2_1/n$  in  $\kappa\text{-}\alpha'_2$ , which leads to a different crystal field acting on the ET molecules in the  $\kappa$  layer. Our tight-binding model parameters for the molecule-based model [Eq. (1) and Table I] provide an adequate and reliable starting point for a many-body description of these systems in terms of a Hubbard-like Hamiltonian where intramolecular


 FIG. 10. (Color online) Comparison of the  $t'/t$  ratios of the three polymorphs which indicate the degree of frustration.

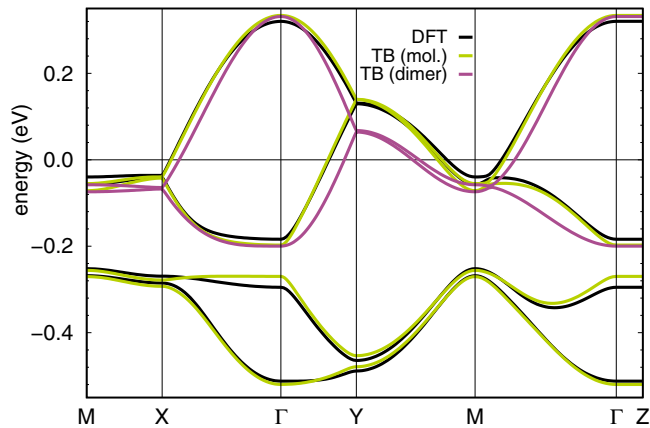


FIG. 11. (Color online) Comparison of an eight parameter molecular TB model to the four parameter dimer TB model for the  $\kappa$  layers of  $\kappa$ - $\alpha'_1$ -(BEDT-TTF)<sub>2</sub>Ag(CF<sub>3</sub>)<sub>4</sub>(TCE).

and intermolecular Coulomb interaction terms should be added to the tight-binding Hamiltonian.

In contrast, an analysis in terms of the simplified dimer model [Eq. (2) and Table IV] shows that the half-filled triangular lattice is not a very good starting point for describing these materials. This is due to the relatively weak dimerization of the (ET)<sub>2</sub> dimers and therefore the contribution of the  $\kappa$  bonding bands should not be neglected when describing the electronic properties of these systems. However, the information obtained from the tight-binding hopping parameters in the dimer model is still useful to roughly classify the degree of frustration in (BEDT-TTF)<sub>2</sub>Ag(CF<sub>3</sub>)<sub>4</sub>(TCE) and have first hints for understanding the different superconducting critical temperatures in these systems. Our comparison of the trends of the frustration parameters with earlier studies shows that the  $\kappa$ -phase system lies in the range of frustration where other  $\kappa$  systems are antiferromagnetic insulators, while the multilayered  $\kappa$ - $\alpha'_1$  and  $\kappa$ - $\alpha'_2$  show a slightly higher frustration degree as also observed in the superconductor  $\kappa$ -(ET)<sub>2</sub>Cu(SCN)<sub>2</sub>. Nevertheless, a detailed understanding of the different critical temperatures requires a many-body analysis of the molecular Hubbard-like model proposed here which is beyond the scope of the present work.

Summarizing, in this work we investigated the electronic properties of the charge-transfer compound (BEDT-TTF)<sub>2</sub>Ag(CF<sub>3</sub>)<sub>4</sub>(TCE). We demonstrated and quantified the importance of the  $\alpha'$  layers with respect to the conducting  $\kappa$  layers and suggested a molecule-based model Hamiltonian to describe these systems. We hope that this work will motivate other groups to investigate these multilayered materials which hold promise of increasing the superconducting critical temperatures in organic charge-transfer superconductors.

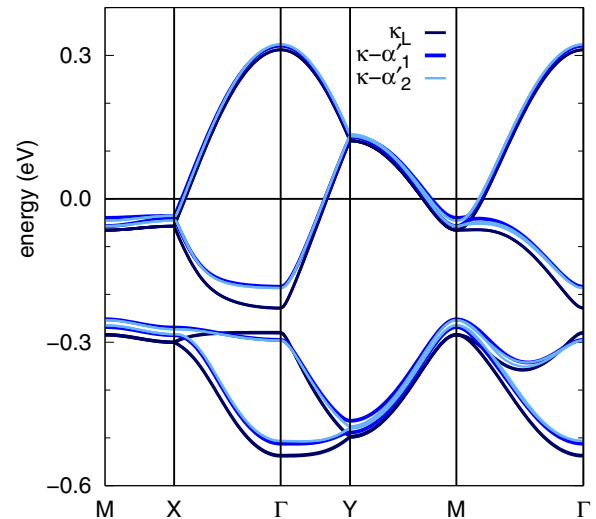


FIG. 12. (Color online) Comparison of the  $\kappa$  bands of the three polymorphs of (BEDT-TTF)<sub>2</sub>Ag(CF<sub>3</sub>)<sub>4</sub>(TCE) on an averaged path through the Brillouin zone (as the in-plane lattice parameters for the three compounds differ slightly).

## ACKNOWLEDGMENTS

We thank D. Guterding and T. Kawamoto for helpful discussions. We acknowledge support by the Deutsche Forschungsgemeinschaft through Grant No. SFB/TR 49 as well as the Center for Scientific Computing in Frankfurt, Germany.

## APPENDIX A: MOLECULE VERSUS DIMER DESCRIPTION

Figure 11 shows a comparison of the DFT calculated  $\kappa$  band structure in the  $\kappa$ - $\alpha'_1$  phase to the molecular TB model based on the eight parameters listed in Table I, and to the dimer TB model based on the four parameters of Table IV. The parameters of the molecule model are calculated using projective Wannier functions, while the dimer model parameters are derived from them via geometrical relations, Eq. (3). It is clear that the dimer model provides only a rough approximation to the two half-filled  $\kappa$  bands at the Fermi level.

## APPENDIX B: COMPARISON OF THE $\kappa$ BANDS OF THE THREE POLYMORPHS

In Fig. 12 we show the  $\kappa$  bands of the three phases of (BEDT-TTF)<sub>2</sub>Ag(CF<sub>3</sub>)<sub>4</sub>(TCE).

- [1] D. Jérôme, *Science* **252**, 1509 (1991).
- [2] H. Mori, *J. Phys. Soc. Jpn.* **75**, 051003 (2006).
- [3] R. S. Manna, M. de Souza, A. Brühl, J. A. Schlueter, and M. Lang, *Phys. Rev. Lett.* **104**, 016403 (2010).
- [4] K. Kanoda and R. Kato, *Annu. Rev. Condens. Matter Phys.* **2**, 167 (2011).

- [5] A. C. Jacko, H. Feldner, E. Rose, F. Lissner, M. Dressel, R. Valentí, and H. O. Jeschke, *Phys. Rev. B* **87**, 155139 (2013).
- [6] T. Mori, *Bull. Chem. Soc. Jpn.* **71**, 2509 (1998).
- [7] T. Mori, H. Mori, and S. Tanaka, *Bull. Chem. Soc. Jpn.* **72**, 179 (1999).
- [8] T. Mori, *Bull. Chem. Soc. Jpn.* **72**, 2011 (1999).

- [9] B. J. Powell and R. H. McKenzie, *J. Phys.: Condens. Matter* **18**, R827 (2006).
- [10] N. Yoshimoto, S. Takayuki, H. Gamachi, and M. Yoshizawa, *Mol. Cryst. Liq. Cryst.* **327**, 233 (1999).
- [11] J. A. Schlueter, K. D. Carlson, U. Geiser, H. H. Wang, J. M. Williams, W.-K. Kwok, J. A. Fendrich, U. Welp, P. M. Keane, J. D. Dudek, A. S. Komosa, D. Naumann, T. Roy, J. E. Schirber, W. R. Bayless, and B. Dodrill, *Physica C* **233**, 379 (1994).
- [12] J. A. Schlueter, L. Wiehl, H. Park, M. de Souza, M. Lang, H.-J. Koo, and M.-H. Whangbo, *J. Am. Chem. Soc.* **132**, 16308 (2010).
- [13] T. Kawamoto, T. Mori, A. Nakao, Y. Murakami, and J. A. Schlueter, *J. Phys. Soc. Jpn.* **81**, 023705 (2012).
- [14] S. D. Obertelli, R. H. Friend, D. R. Talham, M. Kurmoo, and P. Day, *J. Phys.: Condens. Matter* **1**, 5671 (1989).
- [15] I. D. Parker, R. H. Friend, M. Kurmoo, and P. Day, *J. Phys.: Condens. Matter* **1**, 5681 (1989).
- [16] K. Kubo and M. Yamashita, *Crystals* **2**, 284 (2012).
- [17] U. Geiser, J. A. Schlueter, and J. M. Williams, *Acta Crystallogr. B* **51**, 789 (1995).
- [18] T. Kawamoto, T. Mori, T. Terashima, S. Uji, and J. A. Schlueter, *J. Phys. Soc. Jpn.* **82**, 024704 (2013).
- [19] T. Kawamoto (private communication).
- [20] K. Koepf and H. Eschrig, *Phys. Rev. B* **59**, 1743 (1999).
- [21] J. P. Perdew, K. Burke, and M. Ernzerhof, *Phys. Rev. Lett.* **77**, 3865 (1996).
- [22] H. C. Kandpal, I. Ophale, Y.-Z. Zhang, H. O. Jeschke, and R. Valentí, *Phys. Rev. Lett.* **103**, 067004 (2009).
- [23] K. Nakamura, Y. Yoshimoto, T. Kasugi, R. Arita, and M. Imada, *J. Phys. Soc. Jpn.* **78**, 083710 (2009).
- [24] J. Caulfield, W. Lubczynski, F. L. Prat, J. Singleton, D. Y. K. Ko, W. Hayes, M. Kurmoo, and P. Day, *J. Phys.: Condens. Matter* **6**, 2911 (1994).
- [25] J. Ferber, K. Foyevtsova, H. O. Jeschke, and R. Valentí, *Phys. Rev. B* **89**, 205106 (2014).
- [26] P. Guionneau, J. Gaultier, M. Rahal, G. Bravic, J. M. Mellado, D. Chasseau, L. Ducasse, M. Kurmoo, and P. Day, *J. Mater. Chem.* **5**, 1639 (1995).
- [27] H. Eschrig and K. Koepf, *Phys. Rev. B* **80**, 104503 (2009).
- [28] T. Komatsu, N. Matsukawa, T. Inoue, and G. Saito, *J. Phys. Soc. Jpn.* **65**, 1340 (1996).
- [29] M. Tamura, H. Tajima, K. Yakushi, H. Kuroda, A. Kobayashi, R. Kato, and H. Kobayashi, *J. Phys. Soc. Jpn.* **60**, 3861 (1991).